Available online at www.sciencedirect.com

ScienceDirect

Procedia CIRP 82 (2019) 273–278

www.elsevier.com/locate/procedia

17th CIRP Conference on Modelling of Machining Operations

Identification of spindle dynamics by receptance coupling for non-contact excitation system

Orkun Özşahin*[a], Mathieu Ritou[b], Erhan Budak[c], Clément Rabréau[b], Sébastien Le Loch[b]

[a] *Middle East Technical University, Ankara, 06800, Turkey*
[b] *LS2N (Laboratory of Digital Sciences of Nantes, UMR CNRS 6004), University of Nantes, 44000 Nantes, France*
[c] *Manufacturing Research Laboratory, Sabanci University, Tuzla, İstanbul, 81474, Turkey*

* Corresponding author. Tel.: +90 312 210 2568, E-mail address: ozsahin@metu.edu.tr

Abstract

The identification of spindle dynamics plays a crucial role in accurate prediction of the stability diagrams for high speed machining operations. In this study, variations of the mode shapes of the tool-spindle assembly at high spindle speeds are examined using numerical models and hypotheses are formulated. An identification method of spindle dynamics is proposed, dedicated to non-contact excitation system; from which only cross FRF can be obtained (instead of tool tip FRF classically). Then, spindle dynamics is calculated using inverse Receptance Coupling (RC) method. Proposed method enables the identification of the speed dependent spindle dynamics in the full frequency range. The approach has been verified with the Finite Element Model (FEM) of a spindle-bearing assembly. The prediction by RC of the dynamics of another tool has been successfully compared to the FEM simulation.

Peer-review under responsibility of the scientific committee of The 17th CIRP Conference on Modelling of Machining Operations

Keywords: Spindle dynamics, receptance coupling, non-contact excitation.

1. Introduction

Chatter is an important problem in machining operations and can be avoided using stability diagrams [1,2]. In order to determine stability diagrams, tool point FRF should be determined and generally, tool point FRF is obtained for the idle state of the machine. However, under operational conditions dynamics of the spindle-bearing assembly changes due to the centrifugal forces, gyroscopic moments and thermal expansions. Thus, tool point FRFs obtained for the idle state of the machine lead to inaccurate stability predictions.

In order to predict the tool point FRF under operational conditions, there have been both experimental and modeling approaches. Altintas and Cao [3,4] modeled the spindle-bearing assembly including tool, housing, and machine-tool structure dynamics. They used speed dependent bearing model presented by Harris [5]. Advanced models of the preloaded bearing system are also proposed by Rabreau et al. [6]. In addition, Movahhedy and Mosaddegh [7] included the effects of gyroscopic effect in the spindle model. Similarly, Ozsahin et al [8] modeled spindle-holder-tool assembly using analytical solution of Timoshenko beams including gyroscopic moments and centrifugal forces. Modeling approaches showed that main source of deviations is the dynamic changes in the bearings with spindle speed. This is an expected result since bearing stiffness values decrease with increasing speed [4,6,9,10] and bearing dynamics mainly effect the spindle modes of the assembly [11]. In addition to dynamic models, there are also

2212-8271
Peer-review under responsibility of the scientific committee of The 17th CIRP Conference on Modelling of Machining Operations
10.1016/j.procir.2019.04.038

thermo-mechanical models, which include both dynamic and thermal effects [12-14].

Main limitation of the developed models is the difficulties in accurate modeling and in correct updating of detailed spindle-bearing assembly with various contacts. In addition, these models require the detailed geometry of the spindle assembly which is often not available. Therefore, modeling approaches provide an efficient tool for the design and optimization of the spindle-bearing assembly but they lack the accurate prediction of the tool point FRFs.

In addition, there are various experimental approaches for the identification of in-process tool point FRFs such as; operational modal analysis [15], non-contact excitation systems [16-18] and inverse stability identification [19,20].

Main limitation of the experimental approaches is the necessity of the measurements for each holder-tool combinations which is often not possible for machine shop applications. To alter this limitation, Namazi and Altintas [21] proposed an identification method which can be easily applied to idle conditions. Later Grossi et al. [22,23] identified spindle dynamics based on tool point FRFs obtained using inverse stability method. Also, in a recent study, Postel et al. [24] identified speed dependent spindle dynamics using the tool point FRF obtained through inverse stability method.

Inverse stability method provides an efficient and fast method for the identification of in process tool point FRF. In addition, tool point FRF obtained using this approach includes the all possible effects of real machining conditions. However, this approach provides only the deviation of the dominant mode that causes chatter and does not provide the tool point FRF in a wider frequency range. On the other hand, non-contact excitation systems provide the experimental tool-spindle FRFs on large frequency range for any spindle speed, which consequently include all the dynamic effects. A dummy tool with a ferromagnetic core is necessary (e.g. at the height of section 3 in Fig 1). Thus the approach cannot be applied with a real cutting tool. In addition, non-contact excitation system cannot provide the tool tip FRF. Indeed, displacement sensor generally cannot be integrated at the height of the electromagnet, but only at other heights (e.g. sections 2 or 4 in Fig 1). Thus, only cross FRF of dummy tool-spindle can be obtained. Consequently, in order to be able to predict the tool tip FRF a given cutting tool from the spindle dynamics assessed with a non-contact excitation device, a new identification method is required and RC approach seems suitable.

In this study, spindle identification procedure is presented for the non-contact excitation measurements. First, point and cross FRF of the spindle-tool assembly is predicted using the cross FRFs. Then speed dependent spindle dynamics is identified. Proposed method is verified through numerical simulations with a FEM of a spindle-bearing-tool assembly.

2. RC identification with linear interpolation

Spindle dynamics can be identified using the method proposed by Namazi and Altintas [21] where analytically obtained free-free holder-tool assembly dynamics is subtracted from the experimentally measured spindle-holder-tool assembly dynamics. In this approach, to identify the spindle dynamics, point and cross FRFs of the spindle-holder-tool assembly are required and these FRFs can be obtained using impact testing on a stopped spindle. Indeed, impact tests cannot be applied while spindle is rotating at high speeds due to inaccuracy and safety reasons. At this point, non-contact excitation system can be used to measure the FRFs of the rotating spindle-holder-tool assembly. Main limitation of the non-contact excitation measurements is that FRF at the tip cannot be measured using non-contact excitation system. Instead, cross FRF H_{23} and H_{43} (Figure 1) can be obtained experimentally using non-contact excitation systems [18]. However, for the spindle identification, FRFs at tool tip H_{11}, spindle flange H_{55} and across H_{15} are required (Figure 1). In these FRF expressions, first subscript *m* represents the point of response measurement and second subscript *n* represents the point of excitation force.

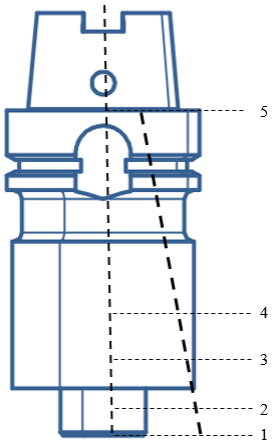

Figure 1. FRF measurement locations and assumed mode shape (black dash line) for the dummy tool.

FRF at any location can be represented as follows:

$$H_{mn} = \sum_{r=1}^{N} \frac{A_{mn}^{r}}{\omega_r^2 - \omega^2 + \mathrm{i}2\xi\omega\omega_r} = \sum_{r=1}^{N} \frac{\phi_r^n \phi_r^m}{\omega_r^2 - \omega^2 + \mathrm{i}2\xi_r\omega\omega_r} \quad (1)$$

where ω_r is the natural frequency of the r^{th} mode, ξ_r is the damping ratio of the r^{th} mode, A_{mn}^{r} is the modal constant, ω is the excitation frequency and ϕ_r^n is the mass normalized r^{th} mode shape at location *n*. Also note that for proportional damping, modal constant will be real and can be expressed as the multiplication of the mass normalized mode shapes as shown in Equation 1.

In order to determine unknown FRFs at location 1 and 5 (H_{11}, H_{15} and H_{55}), ω_r, ξ_r and mass normalized mode shapes at location 1 and 5 (ϕ_r^1, ϕ_r^5) are required.

$$H_{11} = \sum_{r=1}^{N} \frac{\phi_r^1 \phi_r^1}{\omega_r^2 - \omega^2 + \mathrm{i}2\xi_r\omega\omega_r} \quad (2)$$

$$H_{15} = \sum_{r=1}^{N} \frac{\phi_r^1 \phi_r^5}{\omega_r^2 - \omega^2 + i2\xi_r \omega \omega_r} \quad (3)$$

$$H_{55} = \sum_{r=1}^{N} \frac{\phi_r^5 \phi_r^5}{\omega_r^2 - \omega^2 + i2\xi_r \omega \omega_r} \quad (4)$$

Unknown ω_r and ξ_r can be obtained using non-contact excitation measurements since these modal parameters will be same for all FRFs at different locations along the tool axis. On the contrary, mode shapes cannot be directly obtained from these measurements since non-contact measurements will only provide H_{23} and H_{43}. At this point, one common approach might be the constant mode shape assumption where it is assumed that mode shapes will remain the same whatever the spindle speed. Based on that assumption, mode shapes can be identified using impact test on a stopped spindle and assumed as constant at all spindle speeds. However, FEM simulations showed that mode shapes change with spindle speed and this assumption is not valid. Variation of mode shapes with spindle speed is verified in Section 3.3.

In this study, due to the design of the dummy tool (Figure 2), it is proposed to assume as linear the mode shapes of the dummy tool, (in the frequency range of interest) as shown in Figure 1. This is a valid assumption since spindle modes will be dominant for the dummy tool case. Validity of this assumption is also verified using FEM results and these results are also presented in Section 3. Based on this assumption, values of each mode shape at each location can be obtained as follows:

$$\phi_r^3 = C_1, \quad \phi_r^2 = \frac{A_{23}^r}{C_1}, \quad \phi_r^4 = \frac{A_{43}^r}{C_1}$$

$$C_1 = \sqrt{C_2(A_{23}^r - A_{43}^r) + A_{43}^r}$$

$$C_2 = \frac{L_{34}}{L_{34} + L_{32}}$$

where A_{32}^r and A_{34}^r are modal constants identified using measured H_{23} and H_{43}. In addition, L_{34} is the distance between locations 3 and 4, L_{32} is the distance between locations 3 and 2.

Similarly,

$$\phi_r^1 = \frac{\phi_r^3 + (C_3 - 1)\phi_r^4}{C_3}$$

$$\phi_r^5 = \frac{C_4 \phi_r^3 - \phi_r^4}{C_4 - 1}$$

where

$$C_3 = \frac{L_{34}}{L_{34} + L_{32} + L_{12}}$$

$$C_4 = \frac{L_{45}}{L_{45} + L_{34}}$$

Finally, using predicted mass normalized mode shapes (ϕ_r^1 *and* ϕ_r^5) and identified modal parameters (ω_r and ξ_r) point and cross FRFs at locations 1 and 5 can be obtained as using Equations 2-4. Then spindle dynamics can be identified using the method proposed by Namazi and Altintas [21]. In this study FRFs of the free-free dummy tool is obtained using analytical solution of Timoshenko beam equations and receptance coupling method [25]. Then spindle dynamics is identified using predicted spindle-tool assembly FRFs, analytical calculated tool FRFs and inverse receptance coupling method.

3. Verification

3.1. Presentation of FEM model

A Finite Element Model (FEM) of an industrial spindle is used in order to evaluate the identification method proposed in this paper. The spindle is a Fischer MFW 2310, 70 kW, 24 000 RPM; that consists of 5 hybrid angular contact ball bearings (three SKF VEX70 at the front and two VEX60 at the rear) in back-to-back arrangements with two spring preload systems. The main components of the numerical model are presented in Figure 2. The behavior of the angular contact ball bearings is taken into account through a 5DoF stiffness model that depends on spindle speed. The dynamic effects in the bearings are taken into account. Stiffness values are obtained by update of an analytical model of the preloaded spindle axial behavior [6]. The shaft and the dummy-tool are modeled by 3D finite-elements. The HSK interface is considered as rigid. Catia Generative Structural Analysis was used for the simulations of spindle dynamics.

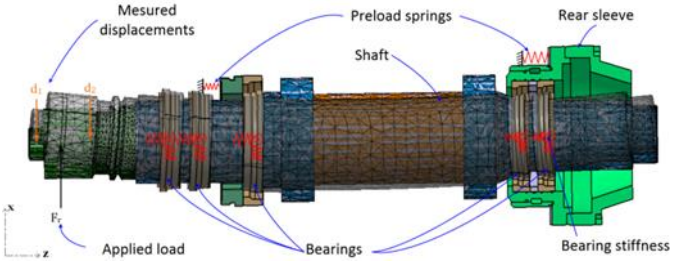

Figure 2. Spindle model for the verifications.

3.2. Identification

In order to verify the proposed method, spindle FEM given in Section 3.1 is used. In FEM, same dummy tool (Figure 1) which is used in non-contact excitation measurements is clamped to spindle-bearing assembly. Then in order to simulate the non-contact measurements, point and cross FRFs (H_{23} and H_{43}) are obtained through FEM at various spindle speeds. The simulated cross FRFs H_{23} are given in Figure 3 at several speeds. Also the natural frequencies identified on the simulated cross FRF are given in Table 1.

As seen from Figure 3 and Table 1, FRF of the spindle-tool assembly changes due to rotational effects and natural frequencies of the system decrease. This is an expected result because, due to gyroscopic moments and centrifugal forces bearing stiffness values decrease with increasing spindle rotational speed [5,6]. Also as expressed by Erturk et al. [25], front and rear bearings mainly effects the spindle and holder

modes. Thus, decrease in the bearing stiffness values result in decrease in the natural frequency of the spindle dominant modes.

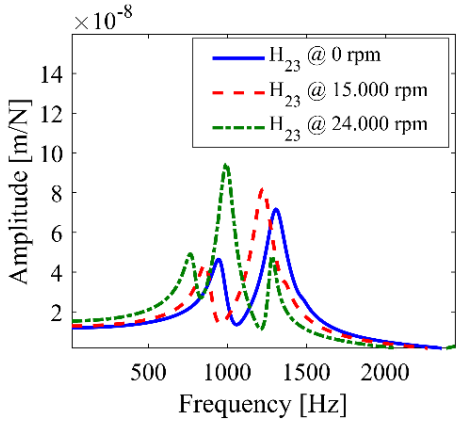

Figure 3. Variation of cross FRF (H_{21}) of the spindle-dummy tool assembly with various spindle speeds.

Table 1 Natural frequencies identified from simulations [Hz]

Mode	0 rpm	15.000 rpm	20.000 rpm	24.000 rpm
1	960.4	873.3	769.5	781.7
2	1308.6	1228.8	914.9	996.4
3	1506.8	1360.9	1270.0	1277.8

3.3. Mode shape evolution with speed

In addition to variations in natural frequencies, modal constants at various spindle speeds are identified using modal analysis (Table 2). One important observation obtained from these simulations is that modal constants thus mode shapes are also effected by the spindle rotational speed. For instance as shown in Table 2, when spindle speed is increased from 0 rpm to 20.000 rpm, modal constant for the first mode A_{12}^{1} decreases to 58% of the idle state. Similarly, there is 27% decrease in modal constant for the second mode when spindle speed is increase from 0 rpm to 20.000 rpm. This is also an expected result, since bearing stiffness variations have different amount of effect on each mode due to the dynamics of the whole system [26].

Table 2 Identified modal constants A_{12}^{r}

	Mode	0 rpm	15.000 rpm	20.000 rpm	24.000 rpm
H_{12}	1	0.1427	0.1034	0.0593	0.0773
	2	0.4725	0.4813	0.3377	0.3432
	3	0.0077	0.0148	0.1282	0.1146

3.4. Validation of linearity hypothesis

As expressed in Section 2, it is assumed that the mode shape of the dummy tool is linear the dummy tool, Consequently, FRF at the tip H_{11} and spindle flange H_{55} (spindle-dummy tool assembly) can be predicted using the mode shape assumption. In order to check the accuracy of the method, cross FRF H_{23} and H_{43} are simulated using the FEM. Then mode shapes are evaluated at locations 1 and 5 using the proposed method. Finally, point and cross FRFs at locations 1 and 5 are calculated. Figure 4 compares the predicted (by RC) and the calculated (FEM) FRF at tool tip H_{11}.

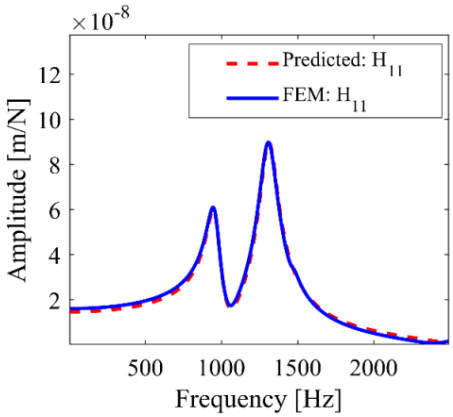

Figure 4. H_{11} for the spindle-dummy tool assembly obtained using FEM and proposed RC method for stopped spindle.

As seen in Figure 4, using the proposed method, unknown point and cross FRFs can be accurately predicted.

In addition to the FRFs, mode shape functions at the tool tip is identified using both the proposed method and FEM. Results are given in Table 3 and as shown in Table 3, linear assumption provides accurate results for the modes in the frequency range of interest. Moreover, mode shapes are examined using FEM and obtained results are given in Figure 5. It illustrates that the first and second modes are mainly spindle modes. These modes show a linear variation in the dummy tool section of the assembly. These results also verify the linear mode shape assumption in the dummy tool section, in the frequency range of interest.

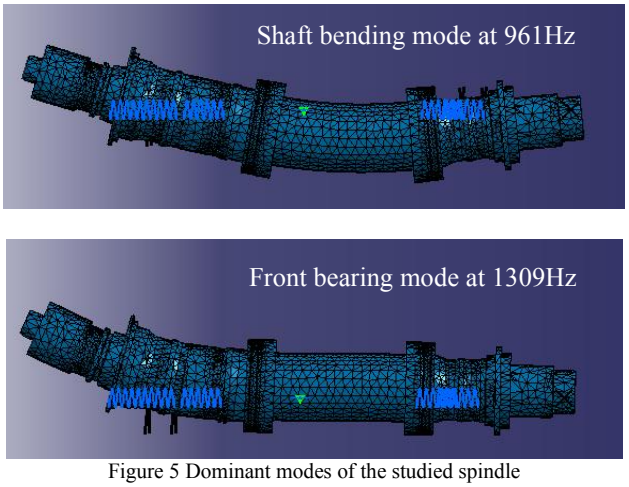

Figure 5 Dominant modes of the studied spindle

Table 3 Modal constants (A_{11}^{r}) at tool tip obtained using FEM and the proposed RC method (for stopped spindle).

Location	Mode	FEM	Predicted	Error (%)
1	1	0.4268	0.4271	0.07
	2	0.7670	0.7679	0.12

4. Results of Receptance Coupling

4.1. Spindle identification

After the prediction of point and cross FRFs of the spindle-tool assembly, dynamics of the dummy tool is subtracted from the dynamics of spindle-tool assembly using the method proposed by Namazi and Altintas [21]. Dynamics of dummy tool at free-free end condition is calculated using the analytical solution of Timoshenko beam and receptance coupling. Identified spindle dynamics H_{55}^{S} (at spindle flange without tool) at different spindle speeds are also given in Figure 6.

There is significant deviation in the spindle dynamics with the increasing spindle speed, which is mainly due to the decrease of bearing stiffness [3]. In addition, deviation in bearing stiffness values increases at high spindle speeds. As can be observed in Figure 6, there is a significant change between 24000rpm and 15000 rpm. Also note that, identified spindle dynamics given in Figure 6, includes the dynamics of spindle, tool portion inside the spindle and effects of the contact mechanism at the spindle-holder flange interface. Contrary to the dummy tool-spindle assembly for which the dominant mode is the font bearing mode (at 1309Hz, Figure 5), the dominant of the identified spindle (without tool) is the shaft bending mode (at 2500Hz).

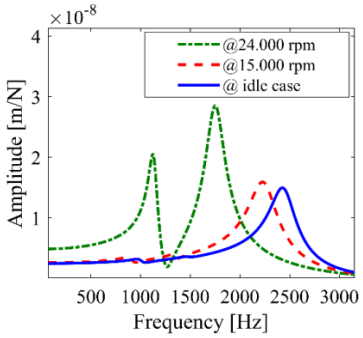

Figure 6. Identified spindle H_{55}^{S} at various speeds.

4.2. Prediction for another tool

In order to verify the accuracy of the identified spindle dynamics, a different tool with a diameter of 32 mm and a length of 175 mm is clamped to the spindle. Then tool point FRF H_{11} is obtained by coupling the identified spindle dynamics (H_{55}^{S}) with the calculated tool dynamics. Tool point and cross FRFs are obtained using FEM for the free-free boundary conditions and then coupled with the identified spindle dynamics using receptance coupling method. In addition, tool point FRF is also calculated using the full spindle-tool FEM. Obtained FRFs H_{11} are given in Figure 7 for various spindle speeds. As shown in Figure 7, tool point FRF of an arbitrary tool can be accurately predicted using the proposed method. The dominant varies from 726 Hz to 688 Hz with speed. Difference between predicted natural frequency of the dominant mode and FEM is 0.69 %, 0.47 % and 0.50 % for the stopped spindle, 15.000 rpm and 24.000 rpm spindle speeds respectively. In addition, for the second mode (at 1042 Hz to 845 Hz), the eigenfrequency is well predicted but the amplitude is overestimated. A possible reason is the assumption of linear mode shape that is less relevant for the second mode, as can be seen in Figure 5.

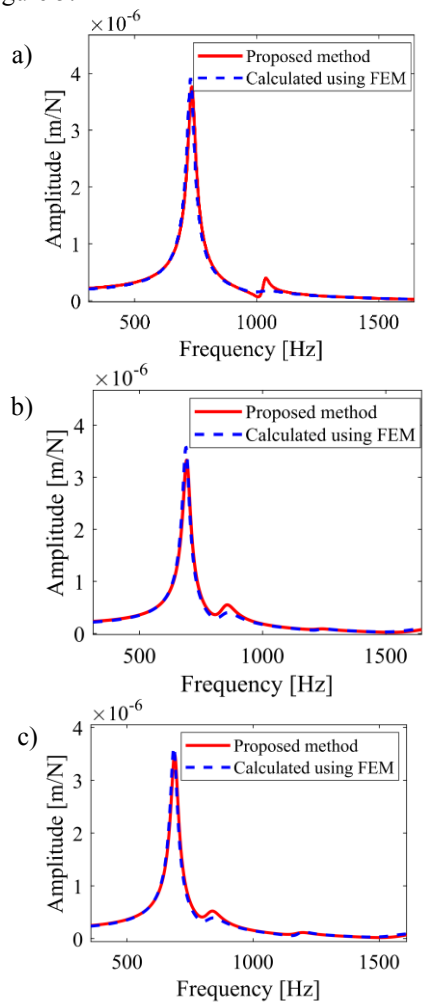

Figure 7. Comparison of tool tip FRF with a different tool, obtained by FEM and by the proposed RC method a) 0 rpm, b) 15000 rpm and c) 24000 rpm.

5. Conclusion

In this paper, a spindle identification method for measurement of non-contact excitation system is presented. In the proposed method, mode shapes of the spindle-tool assembly are considered as speed dependent and determined based on the assumption of linear mode shape of the dummy tool. Validity of this assumption is verified using FEM simulation of an industrial spindle. Based on the FEM results, it is shown that mode shapes changes under operational conditions and their values at the tool tip can be accurately predicted using the proposed method. In addition, spindle dynamics is identified using the proposed method. Then the identified spindle dynamics is coupled with a new tool. The estimation of tool point FRF for the new tool is also validated by the FEM.

References

[1] Y. Altintaş, E. Budak, Analytical Prediction of Stability Lobes in Milling. CIRP Annals - Manufacturing Technology 44 (1995) 357–362.

[2] E. Budak, Y. Altintaş, Analytical Prediction of Chatter Stability in Milling - Part I: General Formulation. Journal of Dynamic Systems, Measurement, and Control 120 (1998) 22–30.

[3] Y. Cao, Y. Altintas, A General Method for the Modeling of Spindle-Bearing Systems, Journal of Mechanical Design 126 (2004) 1089–1104.

[4] Y. Cao, Y. Altintas, Modeling of spindle-bearing and machine tool systems for virtual simulation of milling operations, International Journal of Machine Tools & Manufacture 47 (2007) 1342-1350.

[5] T. A. Harris, Rolling Bearing Analysis, 4th ed., John Wiley and Sons, New York (2001)

[6] C. Rabreau, D. Noel, S. Le Loch, M. Ritou, B. Furet, Phenomenological model of preloaded spindle behavior at high speed, International Journal of Advanced Manufacturing Technology 90 (2017) 3643-3654.

[7] M. R. Movahhedy, P. Mosaddegh, Prediction of chatter in high speed milling including gyroscopic effects, International Journal of Machine Tools & Manufacture 46 (2006) 996-1001.

[8] O. Özşahin, H.N. Özgüven, E. Budak, Analytical modeling of asymmetric multi-segment rotor – bearing systems with Timoshenko beam model including gyroscopic moments, Computers & Structures, 144 (2014) 119-126.

[9] E. Rivin, Stiffness and Damping in Mechanical Design, Marcel Dekker Inc (1999).

[10] B. J. Stone, The state of the art in the measurement of the stiffness and damping of rolling element bearings, CIRP Annals Manufacturing Technology 31 (1982) 529-538.

[11] A. Ertürk, H.N. Özgüven, E. Budak, Effect analysis of bearing and interface dynamics on tool point FRF for chatter stability in machine tools by using a new analytical model for spindle–tool assemblies, International Journal of Machine Tools and Manufacture, 47 (2007) 23-32.

[12] H. Li, Y. C. Shin, Analysis of bearing configuration effects on high speed spindles using an integrated dynamic thermo-mechanical spindle model, Int. J. Mach. Tools Manuf, 44 (2004) 347-364.

[13] C. W. Lin, J. F. Tu, J. Kamman, An integrated thermo-mechanical-dynamic model to characterize motorized machine tool spindles during very high speed rotation, International Journal of Machine Tools & Manufacture 43 (2003) 1035-1050.

[14] C. Rabreau, J. Kekula, M. Ritou, M. Sulitka, J. Shim, S. Le Loch, B. Furet, Influence of bearing kinematics hypotheses on ball bearing heat generation, Procedia CIRP 77 (2018) 622-625.

[15] I. Zaghbani, V. Songmene, Estimation of machine-tool dynamic parameters during machining operation through operational modal analysis, International Journal of Machine Tools and Manufacture 49 (2009) 947-957.

[16] M. Rantatalo, J.O. Aidanpaa, B. Göransson, P. Norman, Milling machine spindle analysis using FEM and non-contact spindle excitation and response measurement, International Journal of Machine Tools and Manufacture 47 (2007) 1034-1045.

[17] A Matsubara, S Tsujimoto, D Kono, Evaluation of dynamic stiffness of machine tool spindle by non-contact excitation tests, CIRP Annals - Manufacturing Technology 64 (2015) 365–368.

[18] D. Tlalolini, M. Ritou, C. Rabréau, S. Le Loch, B. Furet, Modeling and characterization of an electromagnetic system for the estimation of Frequency Response Function of spindle, Mechanical Systems and Signal Processing 104 (2018) 294-304.

[19] N Suzuki, Y Kurata, T Kato, et al., Identification of transfer function by inverse analysis of self-excited chatter vibration in milling operations, Precision Engineering 36 (2012) 568–575.

[20] O Özşahin, E Budak, HN Özgüven, In-process tool point FRF identification under operational conditions using inverse stability solution, International Journal of Machine Tools and Manufacture 89 (2015) 64–73.

[21] M. Namazi, Y. Altintas, T. Abe, N. Rajapakse, Modeling and Identification of Tool Holder – Spindle Interface Dynamics, Int.J. Mach. Tools Manuf 47 (2007) 1333-1341.

[22] Niccolò Grossi, Lorenzo Sallese, Filippo Montevecchi, et al., Speed-varying Machine Tool Dynamics Identification Through Chatter Detection and Receptance Coupling, Procedia CIRP 55 (2016) 77–82.

[23] Grossi, L. Sallese, A. Scippa, et al., Improved experimental-analytical approach to compute speed-varying tool-tip FRF, Precision Engineering, 48 (2017) 114–122.

[24] M Postel, O Özsahin, Y Altintas, High speed tooltip FRF predictions of arbitrary tool-holder combinations based on operational spindle identification, International Journal of Machine Tools and Manufacture, 129 (2018) 48-60.

[25] A. Ertürk, H.N. Özgüven, E. Budak, Analytical modeling of spindle-tool dynamics on machine tools using Timoshenko beam model and receptance coupling for the prediction of tool point FRF, International Journal of Machine Tools and Manufacture 46 (2006) 1901-1912.

[26] M. Ritou, C. Rabréau, S. Le Loch, B. Furet, D. Dumur, Influence of spindle condition on the dynamic behaviour, CIRP Annals - Manufacturing Technology, 67 (2018) 419-422.